JOURNAL OF GUIDANCE, CONTROL, AND DYNAMICS
Vol. 18, No. 1, January–February 1995

Application of Direct Transcription to Commercial Aircraft Trajectory Optimization

John T. Betts* and Evin J. Cramer†
Boeing Computer Services, Seattle, Washington 98124-0346

One of the most effective numerical techniques for the solution of trajectory optimization and optimal control problems is the direct transcription method. This approach combines a nonlinear programming algorithm with a discretization of the trajectory dynamics. When the resulting mathematical programming problem is solved using a sparse sequential quadratic programming algorithm, the technique produces solutions very rapidly and has demonstrated considerable robustness when applied to atmospheric and orbital trajectories. This paper describes the application of the direct transcription technique to the optimal design of a commercial aircraft trajectory, subject to realistic constraints on the aircraft flight path. A primary result of the paper is to demonstrate that the transcription formulation leads to a very natural treatment of realistic Federal Aviation Administration (FAA) imposed path constraints within a high fidelity simulation. A second important result is to demonstrate that modeling tabular data using smooth approximations significantly improves the speed of convergence.

I. Introduction

THIS paper addresses the efficient numerical determination of the flight path of a commercial aircraft described by realistic propulsion, aerodynamic, and atmospheric data when constrained to fly using standard Federal Aviation Administration (FAA) flight regulations. Many portions of the trajectory are prescribed by auxiliary conditions that result in path constraints that are traditionally solved by awkward manipulation. There are two keys to the efficient solution of the problem. The first is the transcription approach, which permits treating the prescribed path conditions in a natural way, as a differential-algebraic equation (DAE) system. The second is the smooth modeling of the tablular data, which results in faster convergence of the optimization without compromising the final answer.

The design of an optimal trajectory for an aircraft has been studied extensively. For example, energy state approximations are described in Refs. 1–3 and singular perturbation techniques have been explored in Refs. 4–6. The presence of singular arcs has also been explored.[7,8] However, realistic path constraints as imposed by standard FAA flight regulations are typically not treated in these analyses. Several researchers have successfully used direct transcription or collocation methods for aerospace applications with path constraints.[9–14] This paper extends their work to a new application.

In the next section we begin with a brief discussion of the optimal control problem and its formulation using direct transcription. We then present the formulation of the aircraft trajectory optimization example, followed by a section that describes a number of mission profiles. After discussing the data modeling problem, a section presenting computational results is given.

II. Trajectory Optimization

A. Optimal Control Problem

There are a number of equivalent ways to state the optimal control problem. To be specific, let us find the n_u-dimensional control vector $\boldsymbol{u}(t)$ to minimize the performance index

$$\phi[\boldsymbol{y}(t_f), t_f] \tag{1}$$

evaluated at the final time t_f, which may be fixed or free. The dynamics of the system are defined by the state equations

$$\dot{\boldsymbol{y}} = \boldsymbol{f}[\boldsymbol{y}(t), \boldsymbol{u}(t), t] \tag{2}$$

where $\boldsymbol{y}$ is the n_e dimension state vector. Initial conditions at time t_0 are defined by

$$\psi[\boldsymbol{y}(t_0), \boldsymbol{u}(t_0), t_0] \equiv \psi_0 = 0 \tag{3}$$

and terminal conditions at the final time t_f are defined by

$$\psi[\boldsymbol{y}(t_f), \boldsymbol{u}(t_f), t_f] \equiv \psi_f = 0 \tag{4}$$

where ψ is a vector of length n_b. In addition, the solution must satisfy path constraints of the form

$$\Psi_L \le \Psi[\boldsymbol{y}(t), \boldsymbol{u}(t), t] \le \Psi_U \tag{5}$$

where Ψ is a vector of size n_p, as well as simple bounds on the state variables

$$\boldsymbol{y}_L \le \boldsymbol{y}(t) \le \boldsymbol{y}_U \tag{6}$$

and control variables

$$\boldsymbol{u}_L \le \boldsymbol{u}(t) \le \boldsymbol{u}_U \tag{7}$$

Note that a path variable equality contraint can be imposed if the upper and lower bounds are equal, e.g., $(\Psi_L)_k = (\Psi_U)_k$ for some k. Portions of a trajectory involving active path constraints form a system of DAEs.

B. Transcription Formulation

The basic approach for solving the optimal control problem by transcription has been presented in detail elsewhere[10–14] and will only be summarized here. All approaches divide the time interval into n_s segments

$$t_0 < t_1 < t_2 < \cdots < t_f = t_{n_s}$$

where the points are referred to as mesh or grid points. Typically grid points are located at a fixed percentage of the total phase time. Let us introduce the notation $\boldsymbol{y}_j \equiv \boldsymbol{y}(t_j)$ to indicate the value of the state variable at a mesh point. In like fashion denote the control at a mesh point by $\boldsymbol{u}_j \equiv \boldsymbol{u}(t_j)$. Many different discretization schemes are

Presented as Paper 92-4528 at the AIAA Guidance, Navigation, and Control Conference, Hilton Head, SC, Aug. 10–12, 1992; received Sept. 1, 1992; revision received Jan. 30, 1994; accepted for publication May 13, 1994.

*Applied Mathematics and Statistics Group. Member AIAA.
†Applied Mathematics and Statistics Group. Senior Member AIAA.

possible and have been compared in Refs. 10 and 11. Each scheme produces a distinct set of nonlinear programming (NLP) variables and constraints. For the reasons described in Refs. 10 and 11, the technique preferred for this application is trapezoidal discretization.

For the trapezoidal discretization, the NLP variables are

$$\boldsymbol{x} = [\boldsymbol{y}_0, \boldsymbol{u}_0, \boldsymbol{y}_1, \boldsymbol{u}_1, \ldots, \boldsymbol{y}_f, \boldsymbol{u}_f, t_f]^\top \tag{8}$$

The state equations (2) are approximately satisfied by setting defects

$$\zeta_j = \boldsymbol{y}_j - \boldsymbol{y}_{j-1} - \tfrac{1}{2}\kappa_j[\boldsymbol{f}_j + \boldsymbol{f}_{j-1}] \tag{9}$$

to zero for $j = 1, \ldots, n_s$. The step size is denoted by $\kappa_j \equiv t_j - t_{j-1}$, and the right-hand side of the differential equations (2) are given by $\boldsymbol{f}_j \equiv \boldsymbol{f}[\boldsymbol{y}(t_j), \boldsymbol{u}(t_j), t_j]$.

As a result of the transcription process, the optimal control constraints (2)–(5) are replaced by the NLP constraints

$$\boldsymbol{c}_L \le \boldsymbol{c}(\boldsymbol{x}) \le \boldsymbol{c}_U \tag{10}$$

where

$$\boldsymbol{c}(\boldsymbol{x}) = [\zeta_1, \zeta_2, \ldots, \zeta_f, \psi_0, \psi_f, \Psi_0, \Psi_1, \ldots, \Psi_f]^\top \tag{11}$$

with

$$\boldsymbol{c}_L = [0, \ldots, 0, \Psi_L, \ldots, \Psi_L]^\top \tag{12}$$

and a corresponding definition of $\boldsymbol{c}_U$. The first $n_e n_s$ equality constraints require that the defect vectors from each of the n_s segments be zero, thereby approximately satisfying the differential equations (2). The boundary conditions are enforced directly by the equality constraints on ψ, and the nonlinear path constraints are imposed at the $n_s + 1$ grid points. Note that nonlinear equality path constraints are accommodated by setting $(\boldsymbol{c}_L)_k = (\boldsymbol{c}_U)_k$ for appropriate values of k. In a similar fashion the state and control variable bounds (6) and (7) become simple bounds on the NLP variables.

C. Nonlinear Programming Problem

The NLP can be stated as follows: Find the N vector $\boldsymbol{x}$ that minimizes the objective function

$$\phi(\boldsymbol{x}) \tag{13}$$

subject to the constraints

$$\boldsymbol{c}_L \le \boldsymbol{c}(\boldsymbol{x}) \le \boldsymbol{c}_U \tag{14}$$

where $\boldsymbol{c}(\boldsymbol{x})$ is an m vector of constraint functions, and the simple bounds

$$\boldsymbol{x}_L \le \boldsymbol{x} \le \boldsymbol{x}_U \tag{15}$$

Equality constraints are imposed by setting $(\boldsymbol{c}_L)_k = (\boldsymbol{c}_U)_k$ and variables can be fixed by setting $(\boldsymbol{x}_L)_k = (\boldsymbol{x}_U)_k$ for appropriate values of k.

Reference 11 presents a nonlinear programming algorithm based on a sparse sequential quadratic programming method. All numerical results presented utilize this algorithm.

III. Problem Formulation

A. Modeling Assumptions

It will be assumed that the aircraft motion is planar, above a flat Earth (i.e., constant gravitational force). All vehicle specific aerodynamic data will be represented by cubic splines with continuity of function, first and second derivatives. We denote the cubic-spline representation of tabular data by $d(\cdot)$ and will describe details of the data modeling below. Similarly, a cubic-spline representation for the *1962 Standard Atmosphere* is used to compute all atmospheric parameters.

The motion of the vehicle will be described by a collection of phases and within each phase a subset of the quantities in Table 1 may be treated as dynamic variables. In general, continuity across events (from one phase to the next) will be maintained for h, r, v, w, and time t. Discontinuities in the lift coefficient C_L and thrust T will be permitted across event boundaries, which is typical for control variables. Discontinuities in the flight path angle γ will be permitted across event boundaries, which is a modeling assumption introduced for consistency with existing vehicle simulations. An alternative approach would be to introduce additional short-duration phases during which the flight path angle changes. However, because the path angle discontinuities are so small, experience suggests the performance degradation attributable to this modeling assumption is negligible.

Table 1 Dynamic variables

h	Altitude, ft
r	Range, nm
v	Velocity, fps
γ	Flight path angle, rad
w	Weight, lb
C_L	Aerodynamic lift coefficient
T	Thrust, lb

B. Equations of Motion

The aircraft dynamics are described by the following set of ordinary differential equations:

$$\dot{h} = v \sin\gamma \tag{16}$$

$$\dot{r} = v \cos\gamma \tag{17}$$

$$\dot{v} = (1/m)(T - D) - g \sin\gamma \tag{18}$$

$$\dot{\gamma} = (1/v)[(L/m) - g \cos\gamma] \tag{19}$$

$$\dot{w} = w_d \tag{20}$$

The propulsive characteristics of the aircraft, namely the total thrust T and total weight flow d_w, are defined by

$$T = m_e d_T(M, h, \tau)\delta \tag{21}$$

$$w_d = m_e d_w(d_T, M, h) \tag{22}$$

where m_e is the number of engines and the thrust of a single engine is given by the trivariate function $d_T(\cdot)$ of Mach number, altitude, and temperature, and the weight flow of a single engine is given as a trivariate function of d_T, Mach number, and altitude. Notice that the atmospheric pressure ratio δ defined below is a correction to the sea-level thrust. We have intentionally used a functional form for the thrust that is consistent with existing vehicle simulations and terminology [cf. Eqs. (2–28) in Ref. 16], even though for a standard atmosphere $\delta = \delta(h)$ and the altitude affect could be incorporated into a modified expression for d_T. It is important to note that Eq. (21) defines the thrust when T is not treated as a control variable. During phases in which thrust is a control variable, Eq. (21) is utilized to define d_T, which will be described below.

The aerodynamic forces on the aircraft are defined by

$$L = C_L q S \tag{23}$$

$$C_D = d_a(C_L, M) + d_R(w, h) + d_0 \tag{24}$$

$$D = C_D q S \tag{25}$$

In these expressions the lift L is defined in terms of the lift coefficient C_L, the dynamic pressure q, and the reference area S. The aerodynamic drag coefficient consists of a basic drag term d_a defined as a bivariate spline involving the lift coefficient and Mach number. The Reynolds number correction d_R is given as a bivariate function of weight and altitude, and d_0 is a constant. The drag D is then given as a function of the drag coefficient, dynamic pressure, and reference area. The atmospheric density $\rho(h)$, pressure $p(h)$, temperature $\tau(h)$, and derivatives $\mathrm{d}\rho/\mathrm{d}h$, $\mathrm{d}p/\mathrm{d}h$, and $\mathrm{d}\tau/\mathrm{d}h$ are all available from the cubic-spline representation of the atmosphere.

In addition the atmosphere also defines the related quantities

$$\delta = (p/p_0) \tag{26}$$

$$M = (v/v_c) \tag{27}$$

$$q = \tfrac{1}{2}\rho v^2 \tag{28}$$

where δ is the pressure ratio, and the Mach number M is computed from the velocity and the speed of sound v_c.

C. Path Constraints

In addition to satisfying the equations of motion, three different types of path constraints will be imposed during various phases of the overall mission. One possibility is to require that the Mach number be constant during a phase, that is,

$$M = (v/v_c) = M_0 \tag{29}$$

where M_0 is the prescribed mach number. Rewriting this as a state variable equality constraint

$$s_M(t) \doteq v - M_0 v_c = 0 \tag{30}$$

Since the control variable C_L does not appear explicitly, let us convert it to a control variable constraint by differentiating,

$$\dot{s}_M(t) = \dot{v} - M_0 \frac{\mathrm{d}v_c}{\mathrm{d}h}\dot{h} = 0 \tag{31}$$

where $\dot{v}$ and $\dot{h}$ are given by the state equations and do contain the control explicitly. Then the original state variable constraint is enforced by imposing $\dot{s}_M(t) = 0$ during the phase, with the boundary condition $s_M(t) = 0$ imposed at one point in the phase, typically either the initial or final point. Notice that when the original path constraint (30) is adjoined to the system of differential equations (16–20), the problem is referred to as a differential-algebraic system with global index 2. In general, the number $\nu - 1$ of differentiations needed to obtain a problem with the control appearing explicitly determines the global index ν (cf. Ref. 17). By differentiating to create a control variable constraint the new DAE system has been converted to have index 1 and is a much more tractable numerical problem.

The second type of path restriction requires a constant rate of climb (or descent) during a phase, that is,

$$\dot{h} = v \sin\gamma = R_0 \tag{32}$$

where R_0 is the desired rate of climb (or sink). Rewriting this expression as a state variable equality constraint yields

$$s_R(t) \doteq v \sin\gamma - R_0 = 0 \tag{33}$$

Since the control variable C_L does not appear explicitly, it is desirable to convert the path constraint to a control variable constraint by differentiating,

$$\dot{s}_R(t) = \dot{v}\sin\gamma + v\cos\gamma\dot{\gamma} = 0 \tag{34}$$

where $\dot{v}$ and $\dot{\gamma}$ are given by the state equations and do contain the control explicitly. As before, we impose $\dot{s}_R(t) = 0$ during the phase, with the boundary condition $s_R(t) = 0$ imposed at one point in the phase.

The third type of path constraint is to require a constant calibrated airspeed (CAS) during a phase, that is,

$$M = C(p, a_0) \tag{35}$$

where a_0 is the desired CAS (knots) and

$$C(p, a_0) = \sqrt{k} \tag{36}$$

$$k = 5[[(k_1/p) + 1]^{\alpha} - 1] \tag{37}$$

where k_1 and α are given constants and p is the atmospheric pressure [cf. Eqs. (1–14) in Ref. 16]. Rewriting yields the state variable equality constraint

$$s_C(t) \doteq v - v_e\sqrt{k} = 0 \tag{38}$$

Again since the control variable C_L does not appear explicitly, we convert the path constraint to a *control variable* constraint and require $\dot{s}_C(t) = 0$, where,

$$\dot{s}_C(t) = \dot{v} - \dot{h}\left(v_c\frac{\mathrm{d}C}{\mathrm{d}p}\frac{\mathrm{d}p}{\mathrm{d}h} + C\frac{\mathrm{d}v_c}{\mathrm{d}h}\right) \tag{39}$$

$$\frac{\mathrm{d}C}{\mathrm{d}p} = \frac{1}{2C}\frac{\mathrm{d}k}{\mathrm{d}p} \tag{40}$$

$$\frac{\mathrm{d}k}{\mathrm{d}p} = -5\alpha\left(\frac{k_1}{p} + 1\right)^{\alpha-1} k_1 p^{-2} \tag{41}$$

$$\frac{\mathrm{d}v_c}{\mathrm{d}h} = \frac{k_2}{2\sqrt{\tau}}\frac{\mathrm{d}\tau}{\mathrm{d}h} \tag{42}$$

where k_2 is a constant, $\dot{v}$ and $\dot{h}$ are given by the state equations, and the atmosphere supplies $\mathrm{d}p/\mathrm{d}h$ and $\mathrm{d}\tau/\mathrm{d}h$.

When one of the path constraints (31), (34), or (39) is adjoined to the equations of motion, we obtain the system of differential algebraic equations

$$\begin{aligned} \dot{\boldsymbol{y}} &= \boldsymbol{f}[\boldsymbol{y}(t), \boldsymbol{u}(t), t] \\ 0 &= \boldsymbol{\Psi}[\boldsymbol{y}(t), \boldsymbol{u}(t), t] \end{aligned} \tag{43}$$

One traditional approach for solving a coupled system such as this is to first solve the path constraint for the control, i.e., attempt to define

$$\boldsymbol{u}(t) = \boldsymbol{\Psi}^{-1}[\boldsymbol{y}(t), t] \tag{44}$$

If this inverse can be computed, then the control can be substituted into the state equations to yield

$$\dot{\boldsymbol{y}} = \boldsymbol{f}[\boldsymbol{y}(t), \boldsymbol{\Psi}^{-1}[\boldsymbol{y}(t), t], t] \tag{45}$$

which is a system of differential equations amenable to solution using a standard initial-value method (e.g., Runge-Kutta). Unfortunately it is often difficult or impossible to construct the inverse $\boldsymbol{\Psi}^{-1}$ analytically. In fact, for the path constraint (31), (34), or (39) this requires inverse interpolation of the aerodynamic data. Direct treatment of the DAE system using the transcription approach avoids this unnecessary and cumbersome process.

D. Cruise Phases

The dynamics of the system can be simplified considerably for cruise phases. This section describes the types of cruise phases of interest.

1. Constant Mach Cruise

One approach is to fly a constant altitude phase at a constant Mach number. In this situation the $\dot{h}$ state equation (16) is unnecessary. Also constant h requires $\gamma = \dot{\gamma} = 0$, which means that $L = w$. In order to maintain a constant Mach number at a constant altitude, it is necessary that the velocity be constant (i.e., $\dot{v} = 0$). It then follows from Eq. (18) that $T = D$. When thrust and drag are equal, it is not necessary to evaluate the thrust curve fit since from the definition we have

$$d_T = \frac{T}{m_e\delta} \tag{46}$$

and this value can be used as the required input for the weight flow data. Finally since the velocity is constant with $\gamma = 0$, the solution of the range differential equation is trivial, i.e.,

$$r_f = r_0 + v\Delta t \tag{47}$$

where r_0 and r_f are the ranges at the beginning and end of the phase of duration Δt.

Table 2 Summary of phase types

Description	States	Control
Climb/descent (CAS = c)	h, r, v, γ, w	C_L
Climb/descent ($M = c$)	h, r, v, γ, w	C_L
Climb/descent (ROC = c)	h, r, v, γ, w	C_L
Cruise ($h = c$, $M = c$)	w	0
Cruise acceleration/deceleration ($h = c$)	r, v, w	0
Maximum range cruise (MRC)	r, v, w	T

2. Acceleration / Deceleration

During short periods of acceleration or deceleration at a constant altitude, both the $\dot{h}$ and $\dot{\gamma}$ equations are unnecessary, and by implication, $L = w$.

3. Maximum Range Cruise

Instead of choosing the thrust equal to the drag as required for a constant Mach cruise segment, it may be preferable to choose the thrust as an optimal function of time. When the thrust appears linearly in the dynamics, the optimally controlled cruise phase is a singular arc, and this problem has been studied by many authors (cf. Refs. 7 and 8). Unfortunately these singular arc studies permit variation in the altitude that is not permitted for a real aircraft operating under FAA flight regulations. Furthermore, for real propulsion data the differential equations are nonlinear with respect to the control variable T. In particular, if relation (46) is used, the weight flow described by d_w is a nonlinear function of the thrust. Consequently a unique optimal choice for the thrust as a function of time during the cruise phase can be determined. Both the $\dot{h}$ and $\dot{\gamma}$ equations are unnecessary, and by implication, $L = w$. However, $\dot{v} \neq 0$ since in general the control variable $T \neq D$.

A summary of the types of phases is presented in Table 2.

IV. Mission Profiles

To illustrate the approach, a number of typical mission profiles will be presented. The profiles are described in the rest of this section and summarized in Tables 3–5. The tables are organized in five columns. The first column defines the type of phase. The nonlinear programming optimization variables are defined for each phase in the second column of the tables. In general the variables in the table must be interpreted as dynamic variables, i.e., the symbol h implies the set of NLP variables $h(t_k) = h_k$ for $k = 1, \ldots, n_i$, where n_i denotes the number of grid points in phase i. For most phases the only nondynamic variables are the initial time t_{i-1}^+ and/or the final time t_i^-. In general it is assumed that phase i terminates at time t_i^- and begins at time t_{i-1}^+ and separate NLP variables are introduced for both sides of the phase boundary. The number of NLP variables introduced on the phase is defined in the row below the definition of the variables. The optimization contraints are defined in columns 3–5 of the tables. Continuous constraints imposed throughout the phase are defined in column 3. The defect constraints (9) that result from discretization of the differential equations are denoted by $\dot{\boldsymbol{y}} = \boldsymbol{f}[\boldsymbol{y}, \boldsymbol{u}, t]$. The number of NLP constraints introduced on the phase is defined in the row below the definition of the constraints. Constraints imposed at the boundary corresponding to the beginning of the phase are listed in the fourth column, and boundary conditions at the end of the phase are listed in the fifth column. For brevity we have omitted the units on the numerical values shown in the tables. However, by convention, the units are consistent with those shown in Table 1. Calibrated airspeed constraints are stated in knots, whereas rate-of-climb constraints are given in feet per minute.

A. Minimum Fuel

The objective is to maximize the weight of the vehicle at the final point, which is equivalent to minimizing the fuel consumed during the flight. The profile describes the trajectory from a point shortly after takeoff (altitude 1517 ft) to a point shortly before landing (altitude 1929 ft). For this case the only control variable appearing is the lift coefficient C_L and all segments containing the control also have a path constraint. Thus for this mission the only freedom available to define the trajectory is the time to "step" from one cruise altitude to another and the initial-values of the flight path angles for some of the phases. Thus, although the sparse nonlinear programming problem had 587 variables, at the solution there were 581 active constraints and only six degrees of freedom. In essence, the entire trajectory can be described by a sequence of DAEs. We shall refer to this case as the "baseline" profile.

B. Maximum Range

The second case of interest can be described as follows: Maximize the final range of the aircraft for a fixed landing weight using the same climb, cruise, and descent flight path definition. This trajectory can be defined from the previous profile by replacing the constraint on the final range (4310.9 nm) with a constraint on the final weight (279,939 lb) and making the range the objective function.

C. Minimum Takeoff Weight

The third case of interest is defined as follows: Minimize the takeoff weight of the aircraft for a fixed landing weight and range using the same climb, cruise, and descent path definitions. Again this case can be obtained with minor changes to the baseline profile, namely adding the constraint that fixes the final weight (279,939 lb) in the final phase and removing the constraint that fixes the initial weight (378,828 lb).

D. Minimum-Fuel MRC

When the cruise portion of the trajectory is prescribed to be at a fixed Mach number as in the previous cases, there are very few degrees of freedom available to minimize the fuel. In contrast, when the thrust is a control variable during the cruise segments, it is possible to enhance the aircraft performance. The climb and descent portions of the trajectory are the same as the baseline profile; however, the cruise portions are modified as described in Table 4.

A comparison of the MRC cruise phases with the baseline cruise phases reveals a number of important differences. First, the thrust is a control variable during the cruise phases, so the number of degrees of freedom for the MRC problem is much larger than the baseline case. Typically the number of degrees of freedom is approximately the same as the number of grid points during the MRC phases. Since thrust is variable during the cruise, it is also necessary to integrate the range and velocity state equations, and thus the number of defect constraints is increased during the MRC cruise, and the number of state continuity constraints at the ends of the cruise phases also reflects this change. A more subtle change also appears in the step climb (phase 6) between the MRC cruise at 31,000 ft and the MRC cruise at 35,000 ft. The step climb is at a constant Mach number, but the value of the Mach number is equal to that at the end of the first cruise segment. To model this, we introduce a single parametric optimization variable (denoted by p in Table 4) that is just the Mach number for the step climb. We refer to it as "parametric" since it is constant during the step climb, but its value is a variable. To ensure the parametric variable does in fact equal the Mach number, a constraint relating it to the velocity and speed of sound is also introduced.

E. Minimum Fuel with Reserves

When designing a realistic mission, it is also necessary to include sufficient reserve propellant to safely reach an alternate landing site. The mission segments for the contingency portion of the trajectory are similar to those for the primary portion, except, of course, the range and cruise altitudes are different. To illustrate this, we augment the baseline mission with the contingency phases defined in Table 5.

F. MRC Cruise and MRC Reserve

The final case investigated essentially combines the missions of the previous two sections. In particular we maximize the final weight of the aircraft for a fixed takeoff weight using the MRC cruise segments for both the baseline and reserve portions of the trajectory. This case results in the largest NLP problem of those considered, with 1290 optimization variables and 1194 constraints active at the solution, producing a problem with 96 degrees of freedom.

Table 3 Baseline mission profile

Trajectory phase	Optimization variables	Optimization constraints		
		During phase	Initial boundary	Final boundary
1. Climb: CAS = 250, $t_0 \le t \le t_1^-$	$h, r, v, \gamma, w, C_L, t_1^-$	$\dot{y} = f[y, u, t]$ $\dot{s}_C = 0$	$h(t_0) = 1517$ $r(t_0) = 0$ $v(t_0) = v_0$ $w(t_0) = 378828$	$h(t_1^-) = 10000$
	$5n_1 + n_1 + 1$	$5(n_1 - 1) + n_1$	4	1
2. Climb: ROC = 500, $t_1^+ \le t \le t_2^-$	$h, r, v, \gamma, w, C_L, t_1^+, t_2^-$	$\dot{y} = f[y, u, t]$ $\dot{s}_R = 0$	$h(t_1^-) = h(t_1^+)$ $r(t_1^-) = r(t_1^+)$ $v(t_1^-) = v(t_1^+)$ $w(t_1^-) = w(t_1^+)$ $t_1^- = t_1^+$ $s_R(t_1^+) = 0$	$t_2^- - t_1^+ \ge 10$
	$5n_2 + n_2 + 2$	$5(n_2 - 1) + n_2$	6	1
3. Climb: CAS = 314, $t_2^+ \le t \le t_3^-$	$h, r, v, \gamma, w, C_L, t_2^+, t_3^-$	$\dot{y} = f[y, u, t]$ $\dot{s}_C = 0$	$h(t_2^-) = h(t_2^+)$ $r(t_2^-) = r(t_2^+)$ $v(t_2^-) = v(t_2^+)$ $w(t_2^-) = w(t_2^+)$ $t_2^- = t_2^+$ $s_C(t_2^+) = 0$	$t_3^- - t_2^+ \ge 10$
	$5n_3 + n_3 + 2$	$5(n_3 - 1) + n_3$	6	1
4. Climb: Mach = 0.8, $t_3^+ \le t \le t_4^-$	$h, r, v, \gamma, w, C_L, t_3^+, t_4^-$	$\dot{y} = f[y, u, t]$ $\dot{s}_M = 0$	$h(t_3^-) = h(t_3^+)$ $r(t_3^-) = r(t_3^+)$ $v(t_3^-) = v(t_3^+)$ $w(t_3^-) = w(t_3^+)$ $t_3^- = t_3^+$	$h(t_4^-) = 31000$ $s_M(t_4^-) = 0$ $t_4^- - t_3^+ \ge 10$
	$5n_4 + n_4 + 2$	$5(n_4 - 1) + n_4$	5	3
5. Cruise: Mach = 0.8, $h(t) = 31{,}000$, $t_4^+ \le t \le t_5^-$	w, t_4^+, t_5^-	$\dot{y} = f[y, u, t]$	$w(t_4^-) = w(t_4^+)$ $t_4^- = t_4^+$	$t_5^- - t_4^+ \ge 10$
	$n_5 + 2$	$n_5 - 1$	2	1
6. Climb: Mach = 0.8, $t_5^+ \le t \le t_6^-$	$h, r, v, \gamma, w, C_L, t_5^+, t_6^-$	$\dot{y} = f[y, u, t]$ $\dot{s}_M = 0$	$w(t_5^-) = w(t_5^+)$ $t_5^- = t_5^+$ $h(t_5^+) = 31{,}000$ $s_M(t_5^+) = 0$ $r(t_5^+) = r(t_4^-) + v_5(t_5^- - t_4^+)$	$h(t_6^-) = 35{,}000$ $t_6^- - t_5^+ \ge 10$
	$5n_6 + n_6 + 2$	$5(n_6 - 1) + n_6$	5	2
7. Cruise: Mach = 0.8, $h(t) = 35{,}000$, $t_6^+ \le t \le t_7^-$	w, t_6^+, t_7^-	$\dot{y} = f[y, u, t]$	$w(t_6^-) = w(t_6^+)$ $t_6^- = t_6^+$	$t_7^- - t_6^+ \ge 10$
	$n_7 + 2$	$n_7 - 1$	2	1
8. Cruise: Decelerate at idle thrust, $h = 35{,}000$, $t_7^+ \le t \le t_8^-$	r, v, w, t_7^+, t_8^-	$\dot{y} = f[y, u, t]$	$w(t_7^-) = w(t_7^+)$ $t_7^- = t_7^+$ $s_M(t_7^+) = 0$ $r(t_7^+) = r(t_6^-) + v_7(t_7^- - t_6^+)$	$s_C(t_8^-) = 0$ $t_8^- - t_7^+ \ge 1$
	$3n_8 + 2$	$3(n_8 - 1)$	4	2
9. Descent: CAS = 250, $t_8^+ \le t \le t_9^-$	$h, r, v, \gamma, w, C_L, t_8^+, t_9^-$	$\dot{y} = f[y, u, t]$ $\dot{s}_C = 0$	$h(t_8^+) = 35{,}000$ $r(t_8^-) = r(t_8^+)$ $v(t_8^-) = v(t_8^+)$ $w(t_8^-) = w(t_8^+)$ $t_8^- = t_8^+$	$h(t_9^-) = 1929$ $r(t_9^-) = 4310.9$ $t_9^- - t_8^+ \ge t_p$
	$5n_9 + n_9 + 2$	$5(n_9 - 1) + n_9$	5	3

Table 4 MRC cruise profile

Trajectory phase	Optimization variables	Optimization constraints		
		During phase	Initial boundary	Final boundary
5. Cruise: MRC, $h(t) = 31{,}000$, $t_4^+ \le t \le t_5^-$	r, v, w, T, t_4^+, t_5^-	$\dot{y} = f[y, u, t]$	$r(t_4^-) = r(t_4^+)$ $v(t_4^-) = v(t_4^+)$ $w(t_4^-) = w(t_4^+)$ $t_4^- = t_4^+$	$t_5^- - t_4^+ \ge 10$
	$3n_5 + n_5 + 2$	$3(n_5 - 1)$	4	1
6. Climb: Mach $= p$, $t_5^+ \le t \le t_6^-$	h, r, v, γ, w, C_L, t_5^+, t_6^-, p	$\dot{y} = f[y, u, t]$ $\dot{s}_M = 0$	$r(t_5^-) = r(t_5^+)$ $v(t_5^-) = v(t_5^+)$ $w(t_5^-) = w(t_5^+)$ $t_5^- = t_5^+$ $h(t_5^+) = 31{,}000$ $p = v(t_5^+)/v_c$	$h(t_6^-) = 35{,}000$ $t_6^- - t_5^+ \ge 10$
	$5n_6 + n_6 + 3$	$5(n_6 - 1) + n_6$	6	2
7. Cruise: MRC, $h(t) = 35{,}000$, $t_6^+ \le t \le t_7^-$	r, v, w, T, t_6^+, t_7^-	$\dot{y} = f[y, u, t]$	$r(t_6^-) = r(t_6^+)$ $v(t_6^-) = v(t_6^+)$ $w(t_6^-) = w(t_6^+)$ $t_6^- = t_6^+$	$t_7^- - t_6^+ \ge 10$
	$3n_7 + n_7 + 2$	$3(n_7 - 1)$	4	1
8. Cruise: Decelerate at idle thrust, $h = 35{,}000$, $t_7^+ \le t \le t_8^-$	r, v, w, t_7^+, t_8^-	$\dot{y} = f[y, u, t]$	$r(t_7^-) = r(t_7^+)$ $v(t_7^-) = v(t_7^+)$ $w(t_7^-) = w(t_7^+)$ $t_7^- = t_7^+$	$s_C(t_8^-) = 0$ $t_8^- - t_7^+ \ge 1$
	$3n_8 + 2$	$3(n_8 - 1)$	4	2

V. Data Modeling

It is common practice to describe the properties of a vehicle by tabular data. Often these data are obtained experimentally (e.g., wind tunnel tests), although in many instances it is simply a convenient form of communication between different engineering disciplines. In any case, the successful use of the data within a numerical process is significantly determined by the method used to represent it mathematically. Recognizing this difficulty is certainly not new and has been discussed by other authors, e.g., Refs. 18 and 19 in the simulation of space launch vehicles. Nevertheless, inappropriate data modeling techniques persist, presumably for historical reasons, in many real applications.

Most state-of-the art numerical methods for integration and optimization require continuity and differentiability in the problem functions. Algorithms based on Newton's method for minimization require that the constraints and objective function be continuous and have first and second derivatives that are continuous. When a cubic B-spline is used to represent tabular data, continuity in the second derivatives can be achieved (cf. Refs. 20–22). However, continuity and differentiability through order 2 is not enough! For rapid optimization convergence, it is also desirable to construct an approximation to the data with "small" values for derivatives above order 2. Loosely speaking we would like to minimize the "wiggle" in the fit. This is desirable because modern optimization methods are predicated upon constructing a quadratic approximation and then solving a sequence of quadratic subproblems. Clearly if the objective and constraint functions are well approximated by a quadratic model, the iterative procedure should converge more rapidly. Conversely, one would expect degraded performance from the optimization algorithm when the functions are dominated by large third and fourth derivatives.

With this in mind, two different methods were used to model the tabular data. Both methods use tensor product B-spline approximations of order 3. Because cubic splines are used, both methods have continuous function, first, and second derivatives, i.e., they are both C^2. The first approach, however, was constructed to interpolate the data. The second method utilized a smoothing spline constructed to minimize the error between the data, with slope and curvature constraints. Of particular importance for this application is the curvature constraint $\partial^2 d_w / \partial T^2 \ge \epsilon$ where acceptable fits were obtained with $\epsilon = 10^{-6}$. Figure 1 displays the second partial derivative of weight flow with respect to thrust for the interpolating cubic spline. In contrast, Fig. 2 displays the same quantity for the smoothing cubic spline. Similar irregularities in the second derivatives were observed for all of the other interpolating data fits. Computational experience with the interpolating and smoothing splines will be presented below.

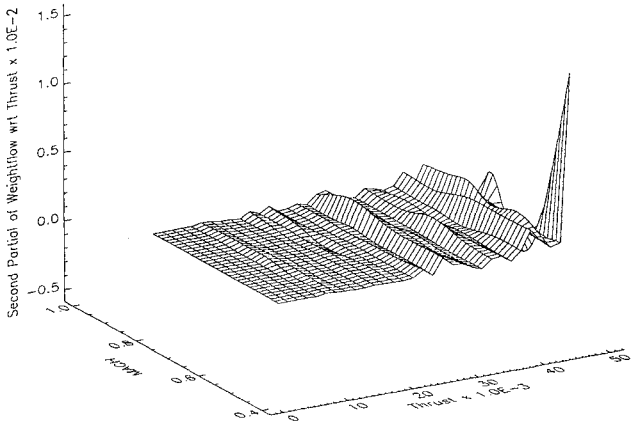

Fig. 1 Curvature variation-interpolating spline.

VI. Computational Results

The nonlinear programming iterations were initialized using a guess for the dynamic variables that was linear between the events. All results were obtained on a SUN IPX workstation using a trapezoidal discretization with an error less that 10^{-3}. Computational

Table 5 Contingency mission profile

Trajectory phase	Optimization variables	Optimization constraints		
		During phase	Initial boundary	Final boundary
10. Climb: CAS = 250, $t_9^+ \le t \le t_{10}^-$	$h, r, v, \gamma, w, C_L, t_9^+, t_{10}^-$	$\dot{y} = f[y, u, t]$ $\dot{s}_C = 0$	$h(t_9^-) = h(t_9^+)$ $r(t_9^-) = r(t_9^+)$ $v(t_9^-) = v(t_9^+)$ $t_9^- = t_9^+$ $w(t_9^+) = w(t_9^-) - 1310$	$h(t_{10}^-) = 10{,}000$ $t_{10}^- - t_9^+ \ge 10$
	$5n_{10} + n_{10} + 2$	$5(n_{10} - 1) + n_{10}$	5	2
11. Climb: ROC = 500, $t_{10}^+ \le t \le t_{11}^-$	$h, r, v, \gamma, w, C_L, t_{10}^+, t_{10}^-$	$\dot{y} = f[y, u, t]$ $\dot{s}_R = 0$	$h(t_{10}^-) = h(t_{10}^+)$ $r(t_{10}^-) = r(t_{10}^+)$ $v(t_{10}^-) = v(t_{10}^+)$ $w(t_{10}^-) = w(t_{10}^+)$ $t_{10}^- = t_{10}^+$ $s_R(t_{10}^+) = 0$	$t_{11}^- - t_{10}^+ \ge 10$
	$5n_{11} + n_{11} + 2$	$5(n_{11} - 1) + n_{11}$	6	1
12. Climb: CAS = 288, $t_{11}^+ \le t \le t_{12}^-$	$h, r, v, \gamma, w, C_L, t_{11}^+, t_{12}^-$	$\dot{y} = f[y, u, t]$ $\dot{s}_C = 0$	$h(t_{11}^-) = h(t_{11}^+)$ $r(t_{11}^-) = r(t_{11}^+)$ $v(t_{11}^-) = v(t_{11}^+)$ $w(t_{11}^-) = w(t_{11}^+)$ $t_{11}^- = t_{11}^+$ $s_C(t_{11}^+) = 0$	$h(t_{12}^-) = 22{,}000$ $t_{12}^- - t_{11}^+ \ge 10$
	$5n_{12} + n_{12} + 2$	$5(n_{12} - 1) + n_{12}$	6	2
13. Cruise: MRC, $h(t) = 22{,}000$, $t_{12}^+ \le t \le t_{13}^-$	$r, v, w, T, t_{12}^+, t_{13}^-$	$\dot{y} = f[y, u, t]$	$r(t_{12}^-) = r(t_{12}^+)$ $v(t_{12}^-) = v(t_{12}^+)$ $w(t_{12}^-) = w(t_{12}^+)$ $t_{12}^- = t_{12}^+$	$t_{13}^- - t_{12}^+ \ge 10$
	$3n_{13} + n_{13} + 2$	$3(n_{13} - 1)$	4	1
14. Cruise: Decelerate at idle thrust, $h = 22{,}000$, $t_{13}^+ \le t \le t_{14}^-$	$r, v, w, t_{13}^+, t_{14}^-$	$\dot{y} = f[y, u, t]$	$r(t_{13}^-) = r(t_{13}^+)$ $v(t_{13}^-) = v(t_{13}^+)$ $w(t_{13}^-) = w(t_{13}^+)$ $t_{13}^- = t_{13}^+$	$s_C(t_{14}^-) = 0$ $t_{14}^- - t_{13}^+ \ge 1$
	$3n_{14} + 2$	$3(n_{14} - 1)$	4	2
15. Descent: CAS = 250, $t_{14}^+ \le t \le t_{15}^-$	$h, r, v, \gamma, w, C_L, t_{14}^+, t_{15}^-$	$\dot{y} = f[y, u, t]$ $\dot{s}_C = 0$	$h(t_{14}^+) = 22{,}000$ $r(t_{14}^-) = r(t_{14}^+)$ $v(t_{14}^-) = v(t_{14}^+)$ $w(t_{14}^-) = w(t_{14}^+)$ $t_{14}^- = t_{14}^+$	$h(t_{15}^-) = 1500$ $r(t_{15}^-) = 4511$ $t_{15}^- - t_{14}^+ \ge t_p$
	$5n_{15} + n_{15} + 2$	$5(n_{15} - 1) + n_{15}$	5	3

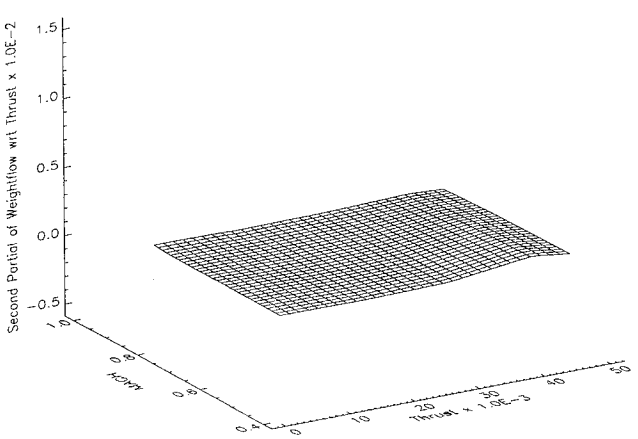

Fig. 2 Curvature variation-smoothing spline.

results were obtained for the six different mission types using both the interpolating and smoothing data described. The results are summarized in Table 6. For each of the cases, we present four pieces of information. The first item is the optimal value of the objective function, i.e., the final range for case 2, the takeoff weight for case 3, and the final weight for all other cases. The second item is the number of function evaluations required to solve the problem, where a function evaluation is defined as an evaluation of the NLP objective function (13) and the NLP constraint vector (14). All gradient and Hessian information was computed using the sparse differencing technique described in Ref. 10, and the total number of function evaluations tabulated includes those needed for finite difference perturbations. The third item tabulated is the number of Hessian evaluations required for convergence. The final item for each case is the total computer time required for solution of the problem. The final column of Table 6 presents the quantity $\%\Delta = 100 \times (i - s)/i$, which is the percent difference between the interpolated data "i" and smooth data "s" results.

First notice that there is essentially no difference in the accuracy of the interpolated vs the smooth results (typically 0.05%). To interpret the remaining performance results, it is important to note that the

Table 6 Performance summary

Item[a]	Interpolating data	Smoothing data	%Δ
	Case 1: minimum fuel, $n_{dof} = 587 - 581 = 6$		
w_f, lb	280,270	280,110	0.057
Fun. ev.	123	140	−13.82
Hes. ev.	1	1	0
Time, s	51.48	55.92	−2.64
	Case 2: maximum range, $n_{dof} = 587 - 581 = 6$		
r_f, nm	1327.73	4319.59	0.188
Fun. ev.	286	286	0
Hes. ev.	5	5	0
Time, s	95.62	93.44	2.28
	Case 3: minimum takeoff weight, $n_{dof} = 587 - 581 = 6$		
w_0, lb	378,395	378,604	−0.055
Fun. ev.	123	140	−13.82
Hes. ev.	1	1	0
Time, s	54.34	55.84	−2.76
	Case 4: minimum fuel $n_{dof} = 813 - 733 = 80$		
w_f, lb	280,875	280,735	0.050
Fun. ev.	1281	424	66.90
Hes. ev.	22	6	72.72
Time, s	357.48	130.51	63.49
	Case 5: minimum fuel with reserves $n_{dof} = 1064 - 1042 = 22$		
w_f, lb	273,467	273,318	0.054
Fun. ev.	601	185	69.22
Hes. ev.	12	2	83.33
Time, s	2478.77	110.58	95.54
	Case 6. MRC cruise, MRC reserves $n_{dof} = 1290 - 1194 = 96$		
w_f, lb	274,065	273,935	0.047
Fun. ev.	1336	483	63.85
Hes. ev.	23	5	78.26
Time, s	588.57	260.99	55.66

[a]Fun. ev. = function evaluation; Hes. ev. = Hessian evaluation.

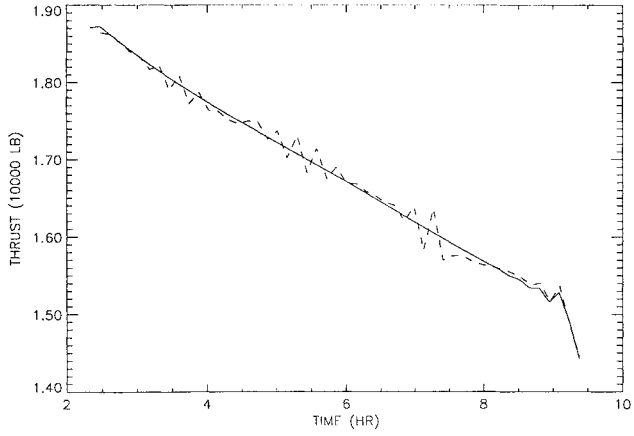

Fig. 3 Thrust history MRC cruise.

first three cases have essentially no degrees of freedom. Even though the NLP has many variables, the number of constraints is also large, and consequently there is little optimization possible! For a problem of this type the Hessian matrix has very little effect. In contrast, cases[4–6] all have a large number of degrees of freedom, due to the presence of the MRC cruise segments. For problems of this type the Hessian matrix is very important, since the progress of the optimization iterations is dictated by the Hessian matrix. Since the purpose of the data smoothing was to reduce Hessian irregularities, the optimization algorithm performed significantly better in these cases. For example in case 4, it was necessary to evaluate the Hessian matrix 22 times and to evaluate the functions 1281 times before the converged solution was obtained (in 357.48 s). However, when the smoothed data were used, the same problem was solved with only 6 Hessian evaluations and 424 function evaluations, producing an overall savings of 63% in computer time. Dramatic improvements were also observed in cases 5 and 6. Although this is not an extensive set of problems, the results strongly suggest that significant benefits accrue from proper modeling of the tabular data!

A second (perhaps more important) benefit can be ascribed to the use of the smooth data and is illustrated in Fig. 3. The shape of the optimal control (thrust-vs-time) history obtained using the smooth data was very "smooth" and well behaved. In contrast, the optimal control history produced by the interpolating data is very erratic and reflects the irregularities in the data modeling.

VII. Summary and Conclusions

This paper describes the application of direct transcription methods to commercial airplane trajectory optimization problems. The applications are characterized by a relatively large number of trajectory phases involving nonlinear path constraints. The path constraints, when adjoined to the state equations, form systems of differential algebraic equations that are solved in a natural, straightforward manner using the transcription method. Treatment of the tabular data describing the aircraft aerodynamics and propulsion was accomplished using tensor product cubic splines. Two different approaches were investigated for constructing the cubic-splines, namely interpolating the data and constructing a least-squares fit subject to curvature constraints. Although both approaches have the necessary continuity and differentiability, the optimization iterations were significantly faster when using the smoothing spline. The overall technique is efficient and robust and permits flexibility in the specification of problem constraints as well as the mission profile.

Acknowledgments

The authors acknowledge the insightful contributions of William Huffman during the development and implementation of this trajectory optimization method. The authors also acknowledge the invaluable assistance of Richard Mastro in the preparation and presentation of tensor product spline models for the vehicle data.

References

[1]Schultz, R. L., "Three-Dimensional Trajectory Optimization for Aircraft," *Journal of Guidance, Control, and Dynamics*, Vol. 13, No. 6, 1990, pp. 936–943.

[2]Bryson, A. E., and Ho, Y. C., *Applied Optimal Control*, Wiley, New York, 1975.

[3]Bryson, A. E., Desai, M. N., and Hoffman, W. C., "Energy-State Approximation in Performance Optimization of Supersonic Aircraft," *Journal of Aircraft*, Vol. 6, No. 6, 1969, pp. 481–488.

[4]Rajan, R., and Ardema, M. D., "Interception in Three Dimensions: An Energy Formulation," *Journal of Guidance, Control, and Dynamics*, Vol. 8, No. 1, 1985.

[5]Calise, A. J., "Singular Perturbation Techniques for On-line Optimal Flight-Path Control," *Journal of Guidance and Control*, Vol. 3, No. 4, 1981, pp. 398–405.

[6]Calise, A. J., and Moerder, D. D., "Singular Perturbation Techniques for Real Time Aircraft Trajectory Optimization and Control," NASA CR-3597, Aug. 1982.

[7]Breakwell, J. V., and Shoee, H., "Minimum Fuel Paths for Given Range," AIAA Paper 80-1660, Aug. 11–13, 1980.

[8]Speyer, J. L., "Nonoptimality of the Steady-State Cruise for Aircraft," *AIAA Journal*, Vol. 14, No. 11, 1976, pp. 1604–1610.

[9]Betts, J. T., and Huffman, W. P., "Trajectory Optimization on a Parallel Processor," *Journal of Guidance, Control, and Dynamics*, Vol. 14, No. 2, 1991, pp. 431–439.

[10]Betts, J. T., and Huffman, W. P., "Application of Sparse Nonlinear Programming to Trajectory Optimization," *Journal of Guidance, Control, and Dynamics*, Vol. 15, No. 1, 1992, pp. 198–206.

[11]Betts, J. T., and Huffman, W. P., "Path Constrained Trajectory Optimization Using Sparse Sequential Quadratic Programming," *Journal of Guidance, Control, and Dynamics*, Vol. 16, No. 1, 1993, pp. 59–68.

[12]Enright, P. J., "Optimal Finite-Thrust Spacecraft Trajectories Using Direct Transcription and Nonlinear Programming," Ph.D. Dissertation, Univ. of Illinois, 1991.

[13]Enright, P. J., and Conway, B. A., "Optimal Finite-Thrust Spacecraft Trajectories Using Collocation and Nonlinear Programming," Paper 89-350, *Proceedings of the AAS/AIAA Astrodynamics Conference*, Stowe, VT, 1989.

[14]Hargraves, C. R., and Paris, S. W., "Direct Trajectory Optimization Using Nonlinear Programming and Collocation," *Journal of Guidance, Control, and Dynamics*, Vol. 10, No. 4, 1987, pp. 338–342.

[15]Hargraves, C. R., Johnson, F., Paris, S., and Rettie, I., "Numerical Computation of Optimal Atmospheric Trajectories," *Journal of Guidance and Control*, Vol. 4, No. 4, 1981, pp. 406–414.

[16]Layton, D. M., *Aircraft Performance*, Matrix, Chesterfield, OH, 1988.

[17]Ascher, U., Mattheij, R., and Russell, R. D., *Numerical Solution of Boundary Value Problems for Ordinary Differential Equations*, Prentice-Hall, Englewood Cliffs, NJ, 1988.

[18]Hallman, W. P., "Smooth Curve Fits for the Shuttle Solid Rocket Booster Data," IOC A85-5752.5-05, Aerospace Corporation, El Segundo, CA, March 1985.

[19]Luke, R. A., "Computational Efficiency Considerations for High-Fidelity Launch Vehicle Trajectory Optimization," AIAA Paper 89-3446, Aug. 1989.

[20]Ferguson, D., and Mastro, R., "Modeling and Analysis of Aerodynamic Data II. Practical Experience," *Proceedings of the AIAA/AHS/ASEE Aircraft Design, Systems and Operations Conference* (Seattle, WA), AIAA Paper 89-2076, 1989.

[21]Ferguson, D., and Mastro, R., "Modeling and Analysis of Aerodynamic Data II," AIAA Paper 89-0476, *Proceedings of the 27th Aerospace Sciences Meeting*, (Reno, NV), AAIA Paper 89-0476, 1989.

[22]Ferguson, D. R., "Construction of Curves and Surfaces Using Numerical Optimization Techniques," *Computer Assisted Design*, Vol. 18, No. 1, 1986.